15th International Symposium on Computer Methods in Biomechanics and Biomedical Engineering
and
3rd Conference on Imaging and Visualization
CMBBE 2018
P. R. Fernandes and J. M. Tavares (Editors)

POINT-OF CARE OLED-BASED MULTIPARAMETRIC BIOCHIP EXPLOITING ADVANCED IMAGE PROCESSING FOR THE DENGUE SEROTYPE RECOGNITION

Patrizia Melpignano*, Serena Morigi†, Enrico Daniso†† , Elena L. Piccolomini† and Luca Benini†

* OR-EL.doo, Volariceva Ulica 6, 5222 Kobarid ,Slovenija
office@or-el-doo.com

† University of Bologna, Dip. Mat., Dip. DISI, Dip. DEI, Bologna, Italy
serena.morigi@unibo.it
elena.loli@unibo.it
luca.benini@unibo.it

†† MP Biomedicals Germany GmbH, Thuringer Strasse 15, 37269 Eschwege, Germany

Keywords: Organic Light Emitting Diode (OLED), Dengue serotypes, CMOS, Image Restoration, Image Segmentation.

Abstract: *As reported by World Health Organization (WHO), most than half of the word population is potentially at risk to be infected with Dengue virus. This virus is a single strained RNA virus of the flaviviridae family that presents four different serotypes. Secondary infections with different serotypes can induce very dangerous complications, like Dengue haemorrhagic fever and shock syndrome. The tropical and sub-tropical areas are the most affected by this infection. Therefore, there is a strong need of a cheap, portable, fast and sensitive diagnostic test also for economic reasons. In this paper, the development of a Point-of-Care multiparametric system using an organic light emitting diode (OLED)-based biochip for the simultaneous detection of the four different Dengue serotypes, is presented. The system exploits the fluorescence detection of a low density matrix of protein antigens and secondary fluorophore tagged antibodies, excited by an OLED source. A low cost CMOS camera, allowing low light detection, to perform multiparametric quantitative analysis has been used in combination with a specifically developed image processing software. The software pipeline adopted is described as well. Fourty Dengue patient sera, previously characterized by standard diagnostic techniques, have been tested, using 3 µl of sera and an incubation time of 30 minutes. The results of these analysis demonstrate the capability of this diagnostic system to perform early Dengue diagnosis and to recognize the Dengue serotype with very high precision, in particular in convalescent patients.*

1 INTRODUCTION

The occurrence of Dengue infectious disease has constantly progressed in the tropical regions of the world starting from the early XX century. A recent report of WHO [28] states that its global annual incidence has been estimated in 50-100 million symptomatic cases in

recent years. However, there is a substantial under-reporting of Dengue within health system and the WHO. Using a cartographic approach, S. Bhatt et al. in 2013 have estimated a global incidence of 390 million cases in the same period. The primary vector of Dengue virus in human transmission is the mosquito Aedes Eagypti which is essentially localized in the tropical and sub-tropical areas of the world. In addition, it has been proven that also the mosquito Aedes Albopictus can sustain the Dengue virus transmission in humans. Due to recent climate changes these mosquitos are rapidly expanding also in Europe and North America and a spread of Dengue outbreaks in these regions is envisaged in the coming years. The Dengue virus is a single strain RNA virus of the flaviviridae family and presents four different serotypes, even if recently a fifth serotype has been identified [21]. The four Dengue serotypes share only about 60/75% of amino acid level and can therefore be considered as distinct viruses [7]. Following a primary Dengue infection with one Dengue serotype, a high titre of neutralizing antibodies is raised giving a long-lasting homotypic protection. However heterotypic protection has a very limited period of time and in case of secondary infection with a different Dengue serotype severe complications can arise (Dengue hemorrhagic fever or Dengue shock syndrome), that can even induce fatality. It is then clear the importance of an early and accurate diagnostic method to determine both the presence of the infection and to understand if it is a primary or a most dangerous secondary infection. Currently the two most commonly used diagnostic methods are the serological and the molecular ones [1,10,24]. Both methods present advantages and disadvantages. While the molecular method (reverse transcriptase polymerase chain reaction, RT-PCR) allows a very early and accurate detection and is able to recognize the infecting serotype, the possibility to use this technique is time limited. The presence of the virus in the sera is normally restricted to 1-3 days after the symptom onset and a delayed blood collection may not allow this kind of diagnosis. Serological diagnostics focus on the detection of IgM and IgG antibodies produced by the immunological system to face the infection. The time evolution of these antibodies is different: the IgM antibodies are present in the sera starting from the fifth/seventh day from the symptom onset and last about three-six month. The IgG antibodies start to be present in the sera after eight/fourteen days from the infection but can be detected for years. It is evident that this kind of diagnostics is not suited for an early diagnosis. Furthermore, in flaviviruses infection there is another important issue to be considered: the cross-reactivity of antibodies against viruses of the same flavivirus family. To circumvent this problem and find a serological diagnostic test suitable also for early diagnostic, the detection of the non-structural protein NS1(glycoprotein) in patient sera has been considered [8,9].While the role of this protein is not completely understood, it is expressed by the infected cells at the very first stage of infection (first day) and seems related to the virus replication [18]. Being NS1 protein specific for the flavivirus that have expressed it, it is less prone to the cross-reactivity issues than standard antibodies. So, currently, RT-PCR and NS1 test offer earlier and more specific diagnostic and are considered the virological proof of infection. In this paper we described a different approach to the serological Dengue diagnostic that have been poorly investigated in the past: the detection of antibodies (both IgM and IgG) against NS1 proteins [27]. Recent investigations showed that IgM anti-NS1 are raised by the immunological system in the very early stage of the infection and presents a good specificity for the specific NS1, while a weak cross-reactivity still persist, in particular in IgG anti-NS1 [13, 27]. Starting from these considerations, we have developed a multi-parametric test for the simultaneous detection of IgM or IgG anti-NS1 using a matrix of the four Dengue specific NS1 proteins in an organic light emitting diode (OLED)-based biochip. The system exploits the fluorescence detection of secondary fluorophore tagged antibodies, excited by an

optimized OLED [16, 17] in an indirect immunofluorescence configuration. For the first time, the use of a CMOS image sensor, in combination with a custom-made image processing software, has allowed to obtain results comparable to a high sensitivity CCD camera. As a result, a very compact, low cost, light i.e. portable, multi-parametric and quantitative Point-of-care device at low price but with sensitivity performances better than standard ELISA diagnostic, has been implemented. The proposed image-processing framework, that will be described in Section 2.5, follows a pipeline strategy which first restores and enhances the low resolution image captured by the CMOS device and then proceeds with an automatic segmentation and diagnostic procedure. In a preliminary work [20], we tested the ability of a similar bio-sensor using a high sensitivity CCD camera for the fluorescent signal detection, to diagnose and recognize the Dengue serotypes using 32 patient sera. This preliminary experiment demonstrated the capability of this test to recognize an early Dengue infection while the serotype recognition was not as accurate. Being the sera samples taken at an unknown stage of the disease we asked for new samples collected at precise time of the disease evolution. The results of these tests have then been compared with the standardized laboratory methods including RT-PCR, Standard Indirect Immunofluorescence (IIF), IgM and IgG ELISA and NS1 ELISA and showed a very high accuracy of our OLED biochip to recognize the Dengue serotype at a convalescent stage of the Dengue disease. Considering that the time analysis is around about 3 minutes and the amount of sera required is 3 µl, the OLED-based PoC could be envisaged as a simple and reliable hand-held PoC test for early Dengue diagnosis and serotype recognition in convalescent stage of the disease (complementary to PCR).

2 MATERIALS AND METHODS

2.1 OLED Fabrication and P.o.C. measurement system

A bottom-emission small molecule-based OLED, which was optimized to obtain a deep-blue (DB) color emission with a peak wavelength of 434 nm [17,19], was used to excite the fluorescence of the commercial dye Alexa Fluor® 430 (Invitrogen, Monza, Italy), with the absorption peak located at 434 nm and the emission peak located at 541 nm [23]. An in-depth physical description and characterization of the patented OLED, adopted in this bio-sensor, using the fluorescent molecule, α-NPD [N, N'-Diphenyl-N, N'-bis (1-naphthylphenyl)-1, 1'-biphenyl-4, 4'-diamine] as an emitter, has been reported by P. Melpignano et al. in [19]. For the fluorescence detection, the disposable bio-chip has been assembled on top of a rectangular DB-OLED together with a high-pass optical excitation filter with a high extinction ratio at the wavelength corresponding to the fluorophore emission (transmission (T) < 10^{-5}) and a high transmission in the excitation spectral region. A second bandpass filter centred on the fluorophore wavelength emission was used before the signal capture camera. The DB-OLED was used at 7.0 Volts with a total optical energy density of 85 µW/cm^2 . A prototype CMOS chip, described in paragraph 2.4, has then been used for the signal acquisition with an integration time of 15 sec.

2.2 Disposable bio-chip fabrication

Our diagnostic point-of-care system adopts an inexpensive disposable cartridge. The cartridge is realized using black plastic and presents a central hole. A highly transparent

polystyrene substrate (T > 90%, thickness 180 μm), chemically functionalized to present a hydrophilic surface, is attached to close the hole obtaining a 150 μl reaction chamber. Four 1μl spots of the four different NS1 Dengue serotype specific recombinant glyco-protein solution (The Native Antigen Company, UK) have then been deposited on the transparent substrate, by a manual pipette. The NS1 protein solutions have been obtained diluting a 0.5 mg/ml NS1 solution in carbonate buffer 1mM at a dilution of 1:50. The four spots have been incubated overnight at room temperature. The positions of the different Dengue NS1 spots on the cartridge transparent substrate are shown in Fig.1 (spots scheme in the Input block).

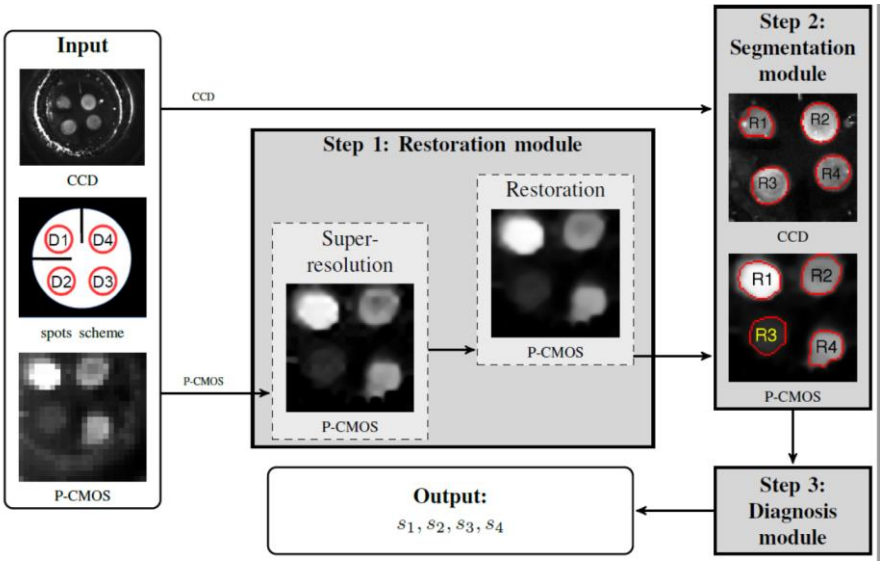

Figure 1: Pipeline of the automatic diagnostic imaging system. The scheme of the Dengue NS1 spot distribution in the plastic cartridge is shown.

2.3 Diagnostics test procedure

In order to detect the presence of IgG and IgM anti-NS1 in the patient sera the following procedure has been adopted. A volume of 150 μl of diluted serum has been put in the reaction chamber in contact with the NS1 protein spots (serum dilution 1:50 in PBS-T, phosphate saline buffer with 0.05% of Tween 20, total amount of sera 3 μl) and incubated at T = 40 C for 15 minutes. In the case of IgM test a preliminary step for IgG removal from the patient serum has been performed. After washing with 150 μl of PBS-T, we performed a second incubation using a 120 μl solution of secondary antibodies (human anti-IgG or anti-IgM) conjugated with fluorophore AlexaFluor 430® (Invitrogen, Monza, Italy) in a dilution of 1:40, starting from a concentration of 2 mg/ml. The human IgG and IgM have been conjugated using the AlexaFluor 430 conjugation kit and following the instructions reported there. After a column purification of the Alexa-conjugated solution, the concentration of the conjugated antibodies in solution has been measured using the spectrophotometer Nanodrop2000c (ThermoFisherScientific,Wilmington, DE, U.S.A.). This second incubation was performed at T = 40 C for 15 minutes. After the final wash, with 150 μl of PBS-T, the dried slide has been measured to detect the fluorescence of the spots and then identify the Dengue anti-NS1 antibodies presence and their reactivity with the serotype specific antigens.

2.4 Detection and image processing

For all the tests the fluorescence signal has been detected using a new CMOS sensor coupled to a miniaturized microscope camera lens. The CMOS sensor has a matrix of 24x24 pixels, 100 μm wide each. It has an optical detection threshold of 10^{-6} lux and a very low (tens of mW) power consumption allowing to power it directly via a USB port (laptop or tablet). The image acquisition integration time can range between 1 ms up to 100 sec. The image digital resolution is at 12 bit (4095 levels). The images are acquired in text format for the successive image processing performed with the software specifically developed for this application.

2.5 Pipeline of the automatic diagnostic imaging system

One critical issue of the adopted CMOS sensor is its low spatial resolution and its relatively high signal noise. The use of large pixel, to improve the optical sensitivity, do not allows to achieve a good spatial resolution and then the CMOS chip can be conveniently used only with low density bio-probe matrices. For this reason, a post-processing phase on an image acquired by a CMOS camera is required to overcome these problems and produce automatic diagnostic results comparable to those produced by a high sensitivity CCD camera. In particular, we followed a pipeline strategy, where in the first phase (restoration) the corrupted image is restored and enhanced, and spatially enlarged by a super-resolution method via compressed sensing strategy. In the second phase, a segmentation procedure allows for the extraction of salient regions of interests in the image, which will be analysed in the third phase in terms of intensity distribution and shape for the identification of the kind of pathogen present and its quantification. In Fig. 1 we illustrate the pipeline of the overall automatic immuno-fluorescent diagnostic imaging system. The image of the same Dengue four spots matrix has been captured both by the high sensitivity CCD camera (Hamamatsu C8484-03G), which represents the ground-truth for the tests, and with the new prototype CMOS chip. We formulate each pipeline stage in a unified variational form. More precisely if u_0 is a given input image, at each stage the output image u* is computed by the minimization of the following functional:

$$u^* = \arg\min_u \{\lambda F(u, u_0) + R(u)\} \quad (1)$$

where $F(u, u_0)$ and $R(u)$ are respectively the data fidelity and regularization component, while $\lambda > 0$ is the trade-off regularization parameter.

The image restoration, segmentation and compressed sensing belong to the mathematical class of inverse problems, which is known to be ill-posed, due to either the non-uniqueness of the solution or the numerical instability of the inversion of the blurring operator in case of image restoration. The regularization term alleviates this problem by reflecting some a-priori properties. In the first phase (restoration) the main noise sources that perturb the images acquired by CMOS sensors, fitting different statistical models, have been considered. In particular, Photo-Response Non-Uniformity (PRNU) is usually modelled as an additive white Gaussian noise; the signal dependent Photon Shot Noise is more properly modelled as a Poisson noise; finally, the ADC noise as an impulsive noise such as the random and salt-and-pepper noise. For the design of the image restoration module, we preliminarily selected and validated the most relevant variational image restoration methods which have been proposed in literature to remove separately the specific blur and noise components identified. The considered methods are: l_2-TV [25], l_1-TV [22], l_p-l_q [15], Non Local Total Variation (NTLV) ([2,12,6]) and Poisson-Gaussian Mixed (PGM) [14]. To overcome the inherent resolution limitations of such low-cost CMOS sensors, a Compressed Sensing (CS) process has been

formulated to generate a 4x super-resolution image via the minimization of the variational functional (1) applying the terms $F(u,u_0)$ and $R(u)$ as described in the Appendix. The second phase (segmentation) plays the important role to automatically recognize the regions with uniform intensity characteristics, such as the fluorescent spots. In our experiments, the images present at most four spots with almost circular shape and different inhomogeneous intensity. Most of the state-of-the art segmentation methods rely on the assumption of constant intra-region intensity, which makes them hardly applicable to our case. To achieve this goal different models have been selected and compared: Chan-Vese (CV) [3], Cai Chan and Zhang (CCZ)[4], and the classical methods such as Region Growing (RG), and Otsu (O). The diagnosis module, illustrated in Fig.1, computes the serological diagnostic for the detection and discrimination of the four different serotypes of the Dengue virus in a set of human samples. The four segmented regions are processed by computing the intensity mean value of the pixels for each region thus identifying both the order of brightness and the concentration associated with each spot. Consequently, the brightest spot intensity allows to determine the specific serotype present in the patient blood.

3 RESULTS AND DISCUSSION

3.1 Quality metrics for image enhancement pipeline

To evaluate the overall system, we introduced some quality metrics and a statistical analysis which allowed us to define the best method combination for the image enhancement pipeline. In the metrics M1 (Sort Matching) the four segmented spots obtained using the CMOS sensor are ordered according to a decreasing concentration (intensity), and compared to the corresponding spots obtained using the CCD camera of the same sample, considering the CCD image as the ground-truth for the test. Let s_i, i=1,..,4, be the calculated concentration in the i-th region, we count the positive matches, thus obtaining a matching score between 0 (no match) and 4 (full match). This score, referred to as M1, is a qualitative index that measures the correct ranking (order) of intensities among regions. In the metrics M2 (Similarity Test), the similarity between the four concentrations detected by CCD and CMOS cameras, is measured by first defining, for each spot, the variation in percentage from the mean value E[s] of the intensities over all the four detected spots, as

$$p_i = \frac{(s_i - E[s]) * 100}{E[s]} \, , i = 1 \dots 4 \tag{2}$$

then computing the displacement between corresponding concentrations in CCD and CMOS acquisitions

$$M_2 = \frac{1}{4} \sum_{i=1}^{4} \left(p_{i,CCD} - p_{i,CMOS} \right)^2 \tag{3}$$

Smaller values for M2 identify better similarity between the two acquisitions. In the metrics M3 (Goodness-of-linear-fit), we investigated if a map between the intensity values on the image captured by the CCD and those significantly lower captured by CMOS exists. For this purpose, we construct the best linear fitting polynomials using regression analysis, then we determine how well the model fits the data by computing the goodness-of-fit R-squared (R2) statistic, also known as coefficient of determination. In particular, we compute the metric M3 as follows:

$$M_3 = \frac{\sum_{i=1}^{4} \left(s_{i,CCD} - \bar{s_i} \right)^2}{\sum_{i=1}^{4} \left(s_{i,CCD} - E[s_{CCD}] \right)^2} \tag{4}$$

where $\overline{s_i}$ is the value predicted by the model in the i-th region. In general, the lower the M3 values, the better the linear model fits the data.

	Metric M1				Metric M2				Metric M3			
	RG	O	CU	CCZ	RG	O	CU	CCZ	RG	O	CU	CCZ
NTVL	87.5	87.5	87.5	**87.5**	123.3	97.6	99.7	**93.1**	0.0068	0.00574	0.00605	**0.0055**
l_1-TV	81.3	81.3	81.3	81.3	122.6	100.5	101.8	98.8	0.00631	0.00616	0.00624	0.00618
l_2-TV	81.3	81.3	81.3	81.3	126.9	102.7	100.2	100.6	0.0075	0.00608	0.00558	0.00596
l_p - l_q	81.3	81.3	81.3	81.3	117.6	99.0	98.4	94.5	0.00651	0.00588	0.00613	0.00609
PGM	81.3	81.3	81.3	81.3	114.4	98.7	99.2	96.4	0.00627	0.00602	0.00606	0.00602
BM3D	81.3	81.3	81.3	81.3	125.8	101.5	101.1	100.5	0.00746	0.00664	0.00655	0.00612

Table 1: Results of the metrics adopted to evaluate the combined performances of the different restoration and segmentation methods compared to the ideal CCD image. Segmentation methods: Region Growing (RG), Otsu (O), Chan-Vese (CU), Cai-Chan-Zeng (CCZ). Restoration methods: Non Local Total Variation (NTLV) [6], l1-TV [22], l2-TV [25], lp-lq [15], Poisson-Gaussian Mixed (PGM) [14] and BM3D algorithm [5].

3.2 Statistics for the metrics considered and models selection

In a preliminarily evaluation phase, we compared the performance of the image restoration models considered, on 200 images synthetically corrupted by both blur effects and additive/multiplicative noise to make them as much as possible similar to the real images. We also included comparisons with the BM3D algorithm, proposed in [5], which is currently one of the most powerful and effective image denoising procedures. This preliminary evaluation phase on synthetic images allowed us to tune at best the free parameters of the compared restoration methods which are then maintained fixed in the restoration of the real images.
On the evaluation of the segmentation methods we compared the results of the segmentation methods previously described with the segmentation results manually obtained by a human expert on the images acquired using the CCD camera in order to define a reference for the comparison. Finally, we analyzed the performance of the restoration and segmentation methods by exhibiting the described statistics. The data set is composed of 16 images related to the detection of the Dengue virus serotypes. Results for the Sort Matching M1 are reported in Table 1 where the values represent the percentages of images that reach the full sort matching (M1=4) for every combination of restoration/segmentation methods. Always in Table 1 we report the results of the Similarity Test M2 metric. We calculated the average value of the whole data set with respect to the restoration and segmentation methods. The best is the lowest value in that it represents the closest reproduction of the human performance on CCD images. The NLTV with CCZ segmentation results to be the best combination but also PGM and *l*p-*l*q methods are competitive. We finally observe that a restoration model with a deblurring component outperforms the BM3D which is a strictly denoising approach. The Goodness-of-linear-fit M3 metric is reported in Table 1-M3. Since the final goal would be to have a function that maps the results produced by a specific kind of device into the CCD results. Even with a modest-size data set the procedure proposed as post-treatment seems to produce results perfectly mappable by a linear map in those obtained by the CCD camera. We can conclude that the NLTV model together with CCZ segmentation seems to be the best working couple of methods, since it respects the right order of intensities for the two cameras, and generally reaches the lowest values in terms of M2 and M3 metrics (Table 1). These two methods have then been suitably integrated in our Immunofluorescent

Diagnostic System which user panel is shown in Fig.2 and that has been used in our Dengue characterization of human sera samples.

IgM Test							**IgG Test**					
	OLED	IIF	OTHER	OLED	IIF	OTHER	OLED	IIF	OTHER	OLED	IIF	OTHER
Pat.n.1	**15-01-2015**			**12-08-2015**			**15-01-2015**			**12-08-2015**		
DEN1	**291**	1:32	PCR TYP 1	**345**	neg	PCR neg	**262**	1:1000	PCR TYP 1	**3053**	1:10000	PCR neg
DEN2	--	1:32	ELISA 62.6	81	neg	ELISA 18.8	--	1:1000	ELISA 44.3	2817	1:10000	ELISA52.4
DEN3	--	1:100	NS1 9.29	140	neg	NS1 neg	--	1:3200	NS1 9.29	2718	1:3200	NS1 neg
DEN4	--	1:32		245	neg		--	1:1000		--	1:3200	
Pat.n. 2	**06-10-2013**			**11-10-2013**			**06-10-2013**			**11-10-2013**		
DEN1	**351**	1:100	PCR neg	271	1:32	PCR TYP2	**441**	> 1:10000	PCR neg	1040	> 1:10000	PCR TYP2
DEN2	184	1:3200	ELISA 60.6	**303**	1:3200	ELISA 56.5	123	> 1:10000	ELISA 54.9	**1044**	> 1:10000	ELISA55.6
DEN3	237	1:32	NS1 8.97	135	1:32	NS1 3.61	289	> 1:10000	NS1 8.97	667	> 1:10000	NS1 3.61
DEN4	--	neg		102	1:10		126	> 1:10000		126	> 1:10000	
Pat. n.3	**26-08-2014**			**04-09-2014**			**26-08-2014**			**04-09-2014**		
DEN1	165	1:32	PCR TYP3	180	1:320	PCR neg	202	1:320	PCR TYP3	2537	1:10000	PCR neg
DEN2	166	1:320	ELISA 62.8	40	1:10000	ELISA 73.9	240	1:3200	ELISA neg	1479	> 1:10000	ELISA42.6
DEN3	**375**	1:320	NS1 9.7	**532**	1:10000	NS1 neg	**532**	1:3200	NS1 9.7	**2571**	> 1:10000	NS1 neg
DEN4	101	1:32		--	1:320		--	1:32		2568	1:10000	
Pat.n.4	**09-05-2014**			**04-06-2014**			**09-05-2014**			**04-06-2014**		
DEN1	--	neg	PCR TYP4	--	neg	PCR neg	--	1:32	PCR TYP4	2700	> 1:10000	PCR neg
DEN2	--	neg	ELISA neg	--	1:32	ELISA 17.4	--	1:32	ELISA 13.2	726	> 1:10000	ELISA50.8
DEN3	--	neg	NS1 9.69	--	1:32	NS1 neg	**306**	1:320	NS1 9.69	922	> 1:10000	NS1 neg
DEN4	--	neg		**1416**	1:1000		--	1:32		**3405**	> 1:10000	

Table 2: Comparison of Dengue sera samples results using different methods. OLED based test (mean of counts in the spot-gray scale [0-4095]),IIF:Indirect Immunofluorescence (cut-off 1:10), PCR for serotype identification, ELISA IgM and IgG (in NTU units, cut-off 9-11 NTU), NS1: ELISA NS1 (cut-off 0.5-1.0)

3.3 Dengue serotype recognition results with characterized human sera

In a preliminary study, 32 samples of Dengue patient sera, previously characterized with PCR, ELISA (IgG and IgM) and NS1 ELISA techniques, have been analyzed. The results of these experiments are extensively reported in reference [20]. A graph with the preliminary results is shown in Fig. 5. The most relevant results of these experiments have been that while a very early detection of the Dengue infected patients is possible by detecting the anti-NS1 IgM antibodies, the serotype recognition seems not very precise in the very early stage of the disease (Fig. 5c, 9 of the 19 identified serotype are not correctly recognized). A more precise recognition of the right serotype seems possible in a convalescent phase of the disease (after the eight/tenth day from the symptoms onset), in particular 10 of the 13 not PCR identified samples are very well recognizable in anti-NS1IgM test. However, in our preliminary work the time of blood sample collection was not reported and the only reference to identify an early stage disease was the virus presence identification by PCR. Then, in order to verify our hypothesis of a best serotype recognition in a convalescent phase of the Dengue disease, we asked to the Institute of Microbiology and Immunology (Faculty of Medicine, University of Ljubljana) a new set of sera samples collected in known different phases of the disease and completely characterized with other standard techniques. In particular, the sera samples used in this experiment have been characterized by the following techniques: ELISA (for anti-virus IgM and IgG detection), Indirect Immunofluorescence IIF (for anti-virus IgM and IgG detection), ELISA NS1 and PCR. The sera samples are from four different serotype Dengue patients.

For our experiments, multiparametric cartridges using the four different serotypes NS1

proteins as antigens deposited in a four spot matrix, as shown in Fig.1, have been used. The spots fluorescence was measured using the CMOS prototype in combination with the described custom developed software for the spot identification and quantification.

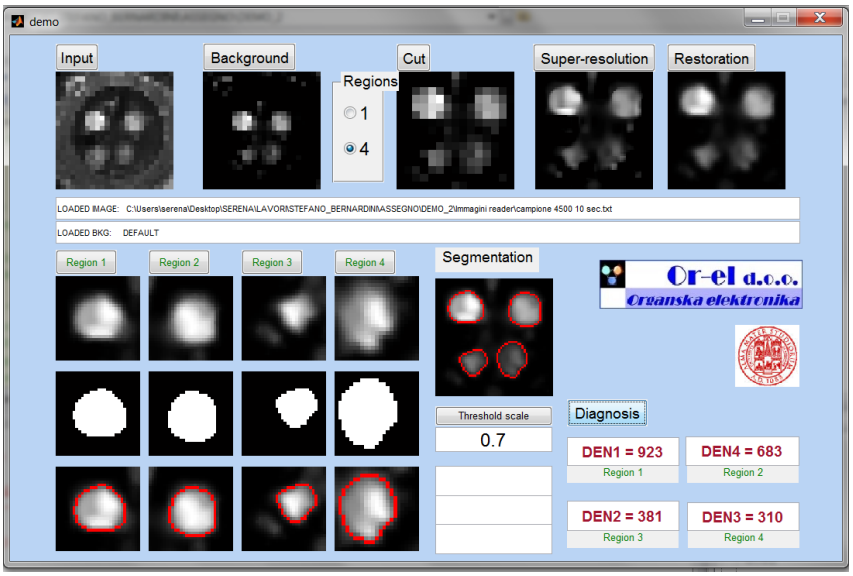

Figure 2: Software interface panel (demo) with the automatic spot recognition and signal digital quantification.

All the fluorescence images have been acquired with a 15 sec. integration time. The acquired images of IgM and IgG tests are shown in Fig. 3 and 4, where the images after the phases of super-resolution, restoration and segmentation are reported. Their numerical results, presented in Tab. 2, were obtained with our point-of-care device (ranging from 0 to 4095 due to the 12-bit image digitalization), and are compared with the results of the previously mentioned standard techniques. As can be seen from Fig.3 a,c,e,g, where the anti-NS1 IgM antibodies are detected, the most part of the investigated samples present an evident cross-reactivity between the different serotype and the serotype identification in this early stage of the disease is not precise in the 50 % of the measured samples. However, the situation changes when the sera of the same patient are collected in a convalescent phase (that in our case range from 5 days to 7 months after the first analysis). As can be seen from Fig. 3 b,d,f,h the serotype identification become more precise also if cross-reactivity persist in some cases. At this stage of the disease, the serotype identification of all our measured sera correspond to the right serotype measured with PCR. It is also evident from the results of the IIF analysis in Tab. 2 that there is not always a correspondence between the results of the detection of anti-virus IgM and anti-NS1 IgM, being this second one more precise in the 62% of the cases. In the case of IgG test of the same samples, it is possible to observe that the presence of IgG against anti-NS1 is lower than the presence of anti-virus IgG in the early stage of the disease, while it is still strong enough to allow the discrimination between primary and secondary infections (see the case of patient n. 2 where it is plausible to observe a secondary infection with serotype 2 associated to a primary infection due to serotype1). It is also interesting to note that in the convalescent phase of the disease, while a stronger cross-reactivity than in the case of anti-NS1 IgM is observed, as reported in [13] and [26], it is still possible to discriminate the right serotype, see Fig.4 and Tab.2. Also in this case there is the evidence of a different results as obtained with conventional IIF technique for the detection of anti-virus IgG with a more precise serotype recognition using the anti-NS1 analysis.

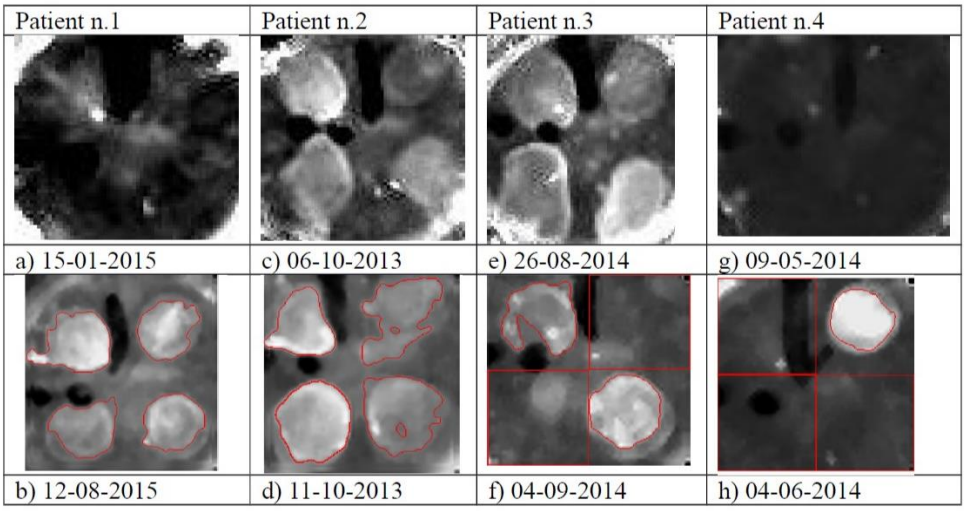

Figure 3: Restored and segmented images of the anti-NS1 IgM test on different patient sera collected at different time of the disease. a),b) Patient n.1 at two different data of sera collection as reported on top of the images., c),d) Patient n.2, e),f) Patient n. 3 and g),h) Patient n.4.

3.4 Test repeatability and cross-reactivity with other flaviviruses

As reported in [20], a first statistical analysis of 20 cartridges prepared with a four spots of NS1-DEN3 antigen, deposited using a manual pipette and used with the same patient serum has allowed to measure an inter and intra assay CV, for an IgG analysis, of respectively 9.4% and 12.7%. Another statistical analysis has also been performed preparing 10 multiparametric cartridges with the four different NS1 antigens, using the same patient serum and measuring the spots intensity with the point-of care device. In this case a CV of 10.1% was measured for the different NS1 spots, being the ratio between the different spots intensity constant in the different trials. We have also measured 10 negative Dengue samples and no fluorescent signal was measured in the four NS1 spot (no images reported). In order to check a possible cross-reactivity with other flaviviruses five samples of human sera positive for West Nile Virus (WNV) and five samples of positive sera for Tick Borne Encephalitis have been tested using the same protocol as described in paragraph 2.3. No cross-reactivity was observed for both anti-NS1 IgM and IgG for the sera of Tick Borne Encephalitis patients, while a very weak signal (on NS1-DEN2 and 3 of around 40 counts) was observed in one WNV patient only for anti-NS1 IgG. No cross- reactivity for anti-NS1 IgM was observed for WNV patients. Then, it is possible to states that, while a better statistic with a higher number of sera samples will be required to validate the diagnostic test, these preliminary results show a very promising ability of the OLED-based bio-sensor to recognize the Dengue serotype in convalescent phase. This possibility could be useful to identify the Dengue serotype in those patients that undergo to a late blood analysis being complementary to a PCR analysis. A further study is envisaged, using different strains of NS1 protein, as well as membrane protein, to try to reduce the cross-reactivity effects and improve the serotype recognition.

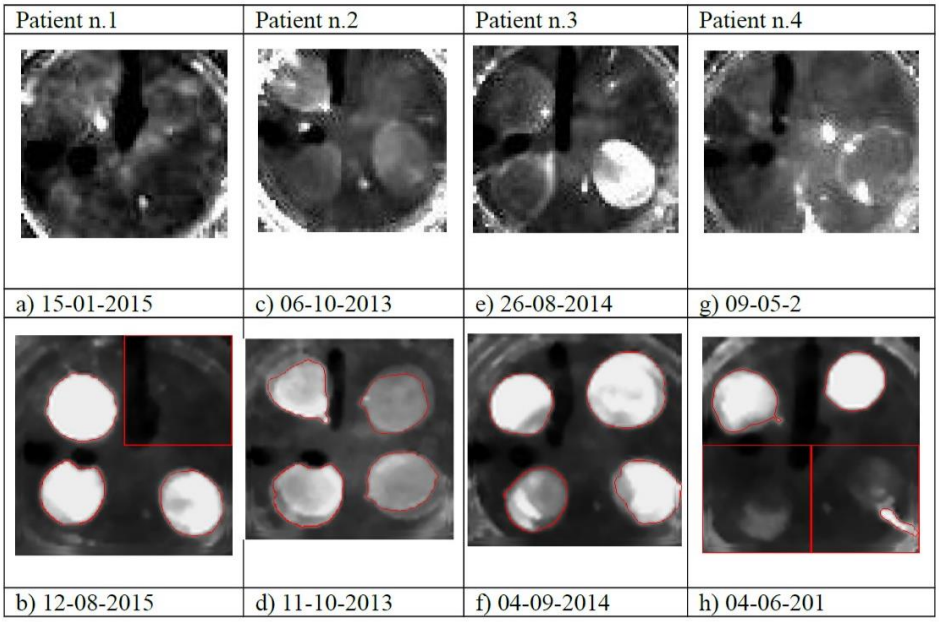

Figure 4: Restored and segmented images of the anti-NS1 IgG test on different patient sera collected at different time of the disease. a),b) Patient n.1 at two different data of sera collection as reported on top of the images., c),d) Patient n.2, e),f) Patient n. 3 and g),h) Patient n.4.

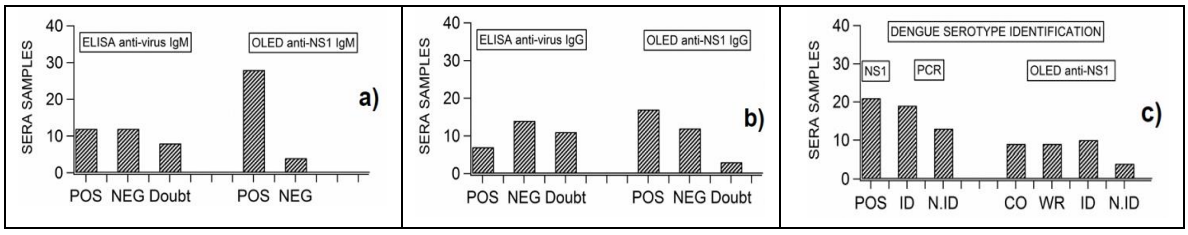

Figure 5: Comparison of the results of the 32 Dengue sera obtained with different analytical methods. A) Positive, Negative and Doubt results obtained with anti-virus IgM ELISA and anti IgM-NS1 OLED tests; b) Positive, Negative and Doubt results obtained with anti-virus IgG ELISA and anti IgG-NS1 OLED tests; c) Serotype identified and not identified samples with PCR technique and Correctly identified samples from the PCR identified, Wrongly identified samples from the PCR identified, Identified from not PCR identified samples and Not identified samples.

4. Conclusions

We have developed for the first time a low cost Point-of-care disposable plastic cartridge reader, based on OLED and low cost CMOS camera, to be used in indirect immuno-fluorescent multi-parametric test. The system has been tested on the simultaneous detection of the four different Dengue serotypes, by using just 3 μl of human sera and with an analysis time around 3 minutes. Thanks to the custom-developed image analysis software, based on variational image enhancement methods, it has been possible to identify and quantify the Dengue serotype present in the patient serum, with a high precision in convalescent phase of the disease. By connecting the portable PoC reader to a USB port of a laptop, or of a tablet, it is possible to obtain a very fast and accurate diagnosis in a few seconds, also thanks to the software interface that allow the fluorescence measure and its quantification. The analysis results are automatically stored in the laptop, as well as the fluorescent image, for recording.

REFERENCES

[1] Blacksell S.D. , Jarman R.G., Gibbons R.V., Tanganuchitcharnchai A., Mammen M.P. Jr. , 2012, Clin Vaccine Immunol 19, 804–810;
[2] Buades A., Coll B., Morel J.M. , 2005, IEEE Computer Society Conference on Computer Vision and Pattern Recognition; 2 : 60-65;
[3] Cai X., Chan R., Zeng T. ,2013, SIAM J. on Imaging Sciences, 2013; 6.1 : 368-390;
[4] Chan T., Vese L., 2001, IEEE Trans. on Image Proc., 10.2 : 266-277;
[5] Dabov K., Foi A., Katkovnik V., Egiazarian K., 2007, IEEE Trans. on Image Proc. 16 (8), 2080-2095;
[6] Gilboa G., Osher S. ,2008, Multiscale Modeling & Simulation , 7.3 : 1005-1028;
[7] Guzmann M.G., Harris E.,2015, Lancet 385 (9966), 453-465;
[8] Hermann L.L., Thaisomboonsuk B. , Poolpanichupatam Y., Jarman R.G., Kalayanarooj S. , Nisalak A. , Yoon I.-K , Fernandez S. , 2014, PLOS Negl. Trop. Dis., 8;
[9] Huang J. L. , Huang J.H ., Shyu R.H , Teng C.W. , Lin Y.L.,Kuo M.D.,.Yao C.W. , Shaio M.F., 2001, Journal of Medical Virology, vol.65, 553 – 560;
[10] Hunsperger E.A., Munoz-Jordan J., Beltran M., Colon C., Carrion J., Vazquez J., Acosta L.N., Medina-Izquierdo J.F., Horiuchi K., Biggerstaff B.J., Margolis H.S., 2016, J. Infect Dis. 214(6):836-44;
[11] Javed A., Kim Y., Khoo M.C.K., Davidson Ward S.L.,Nayak K.S., 2016,IEEE Trans Biomed Eng. , 63/2: 431–437;
[12] Kindermann S, Osher S, Jones PW., 2005, Mult. Mod. & Sim., 4.4 :1091-1115;
[13] Kitai Y., Kondo T., Konishi E., 2011, Journal of Virological Methods, 171:123- 128;
[14] Lanza A., Morigi S., Sgallari F., Wen Y.W., 2014, Computer Methods in Biomechanics and Biomedical Engineering: Imaging & Visualization, 2/1 :12-24;
[15] Lanza A., Morigi S., Reichel L., Sgallari F., 2015, SIAM J. Sci. Comput., 37 : S30-S50;
[16] Manzano M.,Cecchini F., Fontanot M., Iacumin L., Comi G. and Melpignano P., 2015 Biosensors and Bioelectronics, 66: 271-276 ;
[17] Marcello A., Sblattero D., Cioarec C., Maiuri P., Melpignano P., 2013, Biosensors and Bioelectronics, 46: 44-47;
[18] Masrinoul P., Omokoko M.D., Pambudi S.,Ikuta K.,Kurosu T.,2013, Viral Imm., 26;
[19] Melpignano P., Marcello A., Manzano M. and Vidergar N., 2014, Proceeding of the 14th International Symposium on Science and Technology of Lighting (LS14);
[20] Melpignano P. , Daniso E. and Vidergar N., 2016, Informacije Midem, 46/4, 250 – 256 ;
[21] Mustafa M.S.,Rasotgi V.,Jain S.,Gupta V.,2015, Med. J. Arm. Forces India,71(1), 67-70;
[22] Nikolova M., Ng M., Tam C.P. ,2013, SIAM J. on Sci. Comput.;35/1: A397–A430;
[23] Panchuk-Voloshina N., Haugland R.P., Bishop-Stewart J., Bhalgat M.K., Millard P.J., Mao F., Leung W.-Y., 1999, J. Histochem. Cytochem. 47/9, 1179-1188;
[24] Peeling R.W.,Artsob H.,Pelegrino J.L., Puchy P.,Cardosa M.J., Devi S., Enria D.A., Farrar J., Gub¬ler D.J., Guzman M.G., Halstead S.B., Hunsperger E., Kliks S., Margolis H.S., Nathanson C.M., Nguyen V.C., Rizzo N., Vázquez S. and Yoksan S., 2010, Nature Reviews Microbiology, S30-S37;
[25] Rudin L.I., Osher S., Fatemi E.,1992, Physica D: Nonlinear Phenomena; 60.1 : 259-268;
[26] Sankar S.G., Balaji T.,Venkatasubramani K.,Thenmozhi V.,Dhananjeyan K.J., Paramasivan R., Tyagi B.K., Vennison S.J., 2014, J.Imm. Methods, 407: 116-119;
[27] Shu P.-Y. ,Chen L.-K.,Chang S.-F., Su C.-L., Chien L.-J. ,Chin C. , Lin T.-H., Huang J.-H., 2004, Journal of Clinical Microbiology, 42: 2489- 2494;
[28] WHO – WEEKLY EPIDEMIOLOGICAL RECORD n. 30, 29 July 2016

Appendix

We briefly describe the best performant variational models for image restoration/super-resolution/segmentation, which have been integrated in our final proposal of Immunofluorescent Diagnostic System by adapting them to the specific hypothesis and nature of our application context.

1) Image restoration by Non Local Total Variation (NLTV) model

The traditional regularization terms are based on local image operators, which denoise and preserve edges very well, but may induce loss of fine structures during the restoration process. In (Gilboa, 2008) the authors formulated the variational framework of NL-means by proposing nonlocal regularizing functionals and the nonlocal operators such as the nonlocal gradient and divergence. Let u_0 be the given noisy image, H is the blur matrix (that we assume to be known and spatial-invariant), then the NLTV model considered is defined as in (1- formula in the main article) with

$$F(u,u_0) = \frac{1}{2}\|H_u - u_0\|_2^2, R(u) = \|f_{NLTV}(u)\|_1 \qquad \text{(B1)}$$

$f: \mathbb{R}^{n^2} \rightarrow \mathbb{R}^{n^2}$ is the (nonlinear) map from the image u to the L2-norm of its non-local gradient field defined as the vector of all partial differences at x, that is

$$\big(u(y) - u(x)\big)\sqrt{w(x,y)},\ \forall y \in \Omega$$

and w(x,y) is the weight function which returns the similarity of image features between two pixels x and y. In our system we solved the minimization problem (1) by the Bregmanized Operator Splitting (BOS) algorithm using the code available at http: www.cs.cityu.edu.hk/xbresson/ucla/index.html.

2)Segmentation model via Cai-Chan-Zeng (CCZ) method

The segmentation method CCZ aims to minimize a convex version of the Mumford-Shah functional by finding an optimal approximation of the image based on a piecewise smooth function. The CCZ method is based on the observation that one can obtain a good segmentation by properly thresholding a smooth approximation of the given image. Thus in the first stage, the method solves a minimization problem of the form (1) with

$$\lambda = (\lambda_1, \lambda_2)^T, \lambda_1, \lambda_2 > 0 \ and$$
$$F(u,u_0) = \frac{1}{2}\|Hu - u_0\|_2^2, R(u) = (\|\nabla(u)\|_2^2, \|u\|_{TV})^T \qquad \text{(B2)}$$

where H can be a blurring operator or simply the identity matrix (in our tests, we consider H = I). Once u is obtained, then in the second stage the segmentation is done by thresholding u into different phases (regions). The advantages of the CCZ method compared with the CV are the following. Convex optimization techniques can be used to provide an efficient and stable solution to the segmentation problem, it is initialization independent and non-supervised (the number of segments is not fixed in advance), that is it does not need to solve the whole problem again when the number of segments required is changed. The MATLAB code for the CCZ algorithm has been kindly provided by the authors.

3) Super-resolution by Compressive Sensing (CS)

Super-resolution image reconstruction offers the promise of overcoming the inherent resolution limitations of the CMOS low-cost imaging sensors allowing better performance of the post-processing image tools. CS theory improves over conventional approaches to generating a super-resolution image. CS is the process of recovery $u \in \mathbb{R}^N$ from $u_0 \in \mathbb{R}^M$ where u_0 and u are the vector forms of the given low-resolution and the unknown high-

resolution images (M << N), respectively. Let $\Phi \in \mathbb{R}^{N\,x\,M}$ be an orthogonal base which represents the random sampling process, i.e. the acquisition mask to pass from the high-resolution to the low resolution image: $u_0 = \Phi u$. The CS process, suited in cases where images are noisy, can be formulated via the minimization of the variational functional (1), with

$$F(u, u_0) = \frac{1}{2} \|\Phi u - u_0\|_2^2 \, , R(u) = \|u\|_{TV} \qquad \text{(B3)}$$

Super-resolution is an extremely ill-posed problem, since for a given low-resolution input u0, infinitely many high-resolution images u satisfies the above reconstruction constraint. We then further regularize the problem via the R(u) prior which imposes the sparsity of the gradient of the images.